

SOVIET PHYSICS

JETP

A translation of the Zhurnal Éksperimental'noi i Teoreticheskoi Fiziki.

Vol. 14, No. 1, pp 1-223

(Russ. orig. Vol. 41. No. 1, pp 3-308, July, 1961)

January, 1962

SECONDARY ION EMISSION FROM METALS INDUCED BY 10 – 100 keV IONS

B. V. PANIN

Submitted to JETP editor September 29, 1960

J. Exptl. Theoret. Phys. (U.S.S.R.) **41**, 3-10 (July, 1961)

Secondary ion emission from Mo, Zr, and graphite bombarded with H_1^+ , H_2^+ , H_3^+ , He^+ , C^+ , N^+ , Cl^+ , Ar^+ , and Mo^+ ions was studied to determine the mechanism of interactions between medium-energy (10 – 100 keV) atomic particles and solids. The dependences of ion-ion emission coefficients on the nature of the primary ions, and on their initial velocity and charge were investigated.

THE study of the mechanism of interactions between atoms or ions with intermediate energies (10 – 100 keV) and solids has acquired increasing importance in recent years, because of the continually expanding utilization of fast ions in widely diversified fields of science and technology. Information is obtained by studying the secondary ion emission induced when solids are bombarded with ions or atoms. This field is very well covered by reviews such as [1] and a number of theories describing ion bombardment processes have recently been proposed.[2-6] The testing of these theories requires new experimental investigations, since conflicting data are often found in the literature. Even relatively recent publications are either inadequate methodologically or discuss narrowly limited special cases.

The shortcomings of these investigations include a) uncontrolled composition and energy of the bombarding particles (as in measurements in connection with a glow discharge); b) insufficiently thorough cleaning of the working surfaces of target (adsorption from the ambient, nonvolatile impurities that can be formed during the production and treatment of the target material or during its thermal conditioning in the measuring apparatus or under ion bombardment); and c) systematic errors in measuring particle emission from the target surface, resulting often from lack of knowledge regarding the mass, charge, and energy

distributions of the particles. The present investigation of some characteristics of ion-ion emission excludes some of these defects, while reducing considerably the influence that the other defects have on the results.

APPARATUS AND EXPERIMENTAL TECHNIQUE

The mass monochromator represented in Fig. 1 was used to produce ions of rigorously defined masses and energies. Different isotopes from H_1^+ to Mo^+ with energies ranging from 5 to 120 keV bombarded 2×5 mm² targets; the resolving power was $m/\Delta m \approx 200$. The ion current density at the target was $10^{-8} - 10^{-3}$ amp/cm². Ion energies were determined from the accelerating potential difference (with 0.01% stabilization) between the electrodes of the ion source. The ion energy spread at the target was under 1%.

Target contamination by atoms from the surrounding space was reduced by lowering residual gas pressure in the chamber of the target 16, and by using hot targets (above 1000°C). A differential pumping system (a series of oil diffusion pumps with "non-leaking" liquid nitrogen traps) and the copper shell 12 at liquid nitrogen temperature reduced the residual gas pressure in the working chamber to $(2 - 3) \times 10^{-8}$ mm Hg.

Metal targets in the form of $30 \times 12 \times 0.2$ mm ribbons and graphite targets 0.4 – 0.5 mm thick

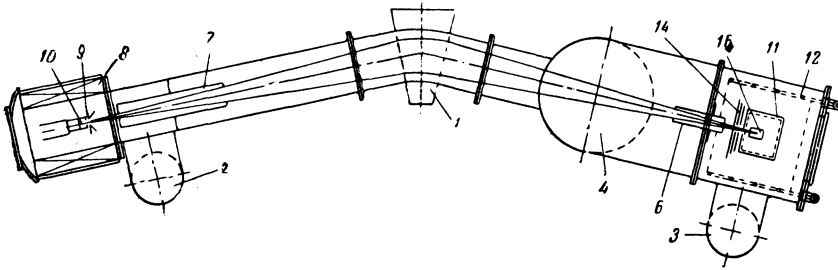


FIG. 1. Diagram of apparatus. 1 – electromagnet; 2, 3 – diffusion pumps; 6, 7 – tubular diaphragms; 8 – solenoid of ion source; 9 – accelerating electrode; 10 – gas-discharge unit of ion source; 11 – secondary-ion collector; 12 – enclosing shell cooled by liquid nitrogen; 14 – three-electrode diaphragm; 16 – target.

were heated by emission from a tungsten-ribbon heater located directly behind the target.

Figure 2 shows the method used to measure ion-ion emission coefficients. A beam of ions with a specified mass and charge was directed at the target 1 through an aperture in the three-electrode diaphragm 11. A 3×3 mm aperture for the purpose of defining the ion-beam cross section was cut in the first electrode, a plate of the same material as the target. This protected the target surface from contamination by foreign atoms produced through sputtering of the edges of the first diaphragm.

The apertures in the second and third electrodes were somewhat larger, so that their edges were not bombarded by ions. These electrodes prevented secondary electrons and ions formed at the edge of the first diaphragm from entering the target-to-collector system. A 400-volt potential was applied to all three electrodes, with alternating signs in a sequence depending on the charge sign of the secondary ion under investigation. The secondary-ion collector was a rectangular chamber surrounding the target 1.

For the purpose of excluding errors in current measurements resulting from tertiary electrons formed on the collector walls, a molybdenum grid was installed on the inner walls of the collector and was given a 150-volt negative potential with respect to the latter. During the measurements of the coefficient δ^+ the potential difference between the target and collector was maintained at -400 v, which when added to the grid potential provided a -550 -volt stopping potential for negative secondary ions.

Analysis of the secondary-ion energy spectra revealed the existence of a considerable number of negative secondary ions with energies above 550 eV. The error thus introduced in the measurement of positive secondary-ion currents was estimated from the secondary-ion energy spectra. In bombardments with ions of atoms (Ar) possessing no electron affinity, attenuation of the positive secondary-ion current cannot exceed 2%. For bom-

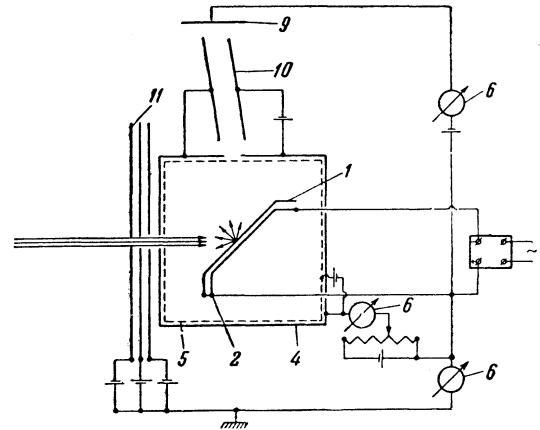


FIG. 2. Experimental arrangement for measuring ion-ion emission coefficients δ^+ . 1 – target; 2 – heater; 4 – ion collector; 5 – grid; 6 – microammeters; 9 – electron collector; 10 – deflecting system; 11 – three-electrode diaphragm.

bardments with O^+ and C^+ this error increases somewhat; for H^+ the error reaches 20%.

The value obtained for δ^+ was also affected by the escape of fast ions of both signs from the measuring system. It follows from geometrical considerations that this error cannot exceed $\pm 1\%$ of the true value of δ^+ ; this error has therefore been neglected. Random errors measured from the spread of the measurements did not exceed $\pm 5\%$ in any instance. All currents were measured with M-95 microammeters having a maximum sensitivity of 2×10^{-9} amp per scale division.

Figure 3 shows three additional electrodes (9 and 10), which were used to determine the negative component δ^- of secondary-ion emission. If the current received by the collector is to consist only of negative secondary ions, it is insufficient to hold positive ions at the target. The negative ions must also be separated from the simultaneous flux of secondary electrons, which is at least ten times greater than the ion flux. For this purpose the entire measuring setup was placed in a magnetic field whose lines of force proceeded from the target 1 through an opening in the collector 4, between the electrodes 10, and through the electrode 9. Consequently, all electrons leaving

FIG. 3. Ion-ion emission coefficient δ^+ for Mo target vs velocity v of bombarding Mo^+ , Ar^+ , Ne^+ , He^+ , H_3^+ , H_2^+ , and H_1^+ ions. For H_3^+ , $\frac{1}{3}\delta$ is given; for H_2^+ , $\frac{1}{2}\delta$ is given.

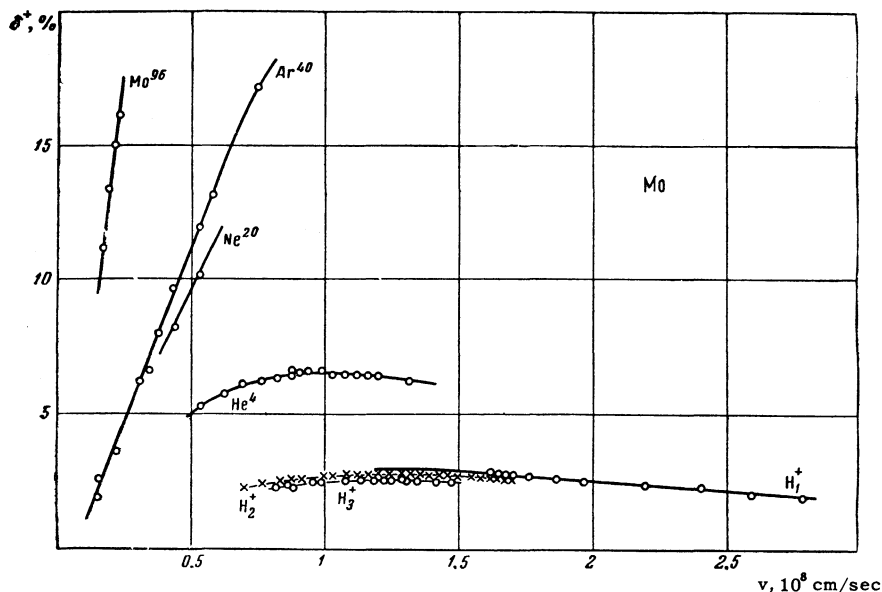
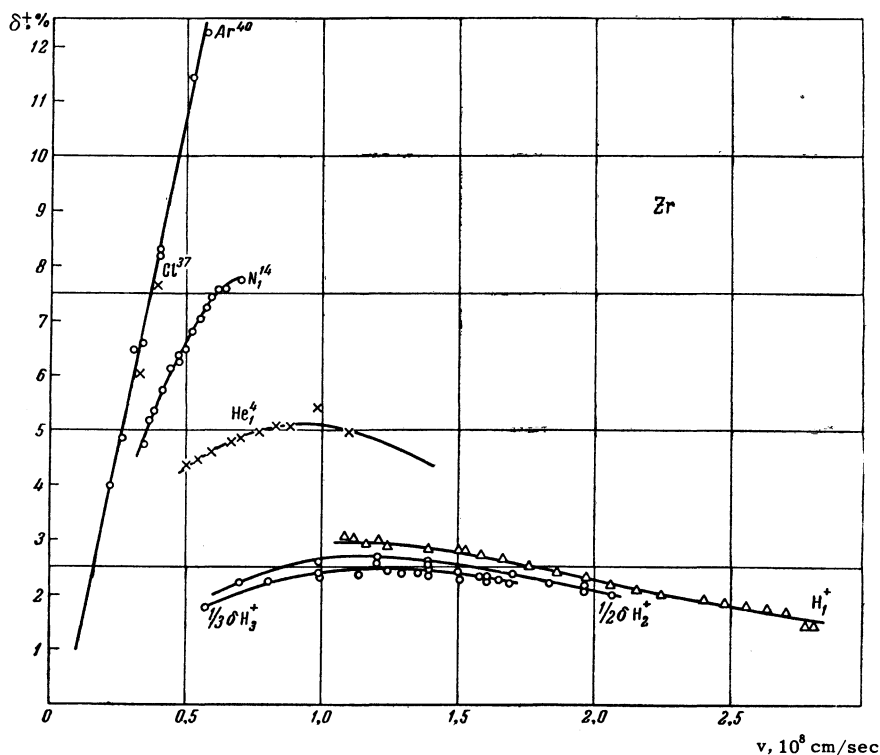


FIG. 4. Ion-ion emission coefficient δ^+ for Zr target vs velocity v of bombarding Ar^+ , Cl^+ , N^+ , He^+ , H_3^+ , H_2^+ , and H_1^+ ions.



the target moved to the electrode 9 along helical trajectories even in relatively weak fields (not stronger than 1000 oe).

A few very slow negative secondary ions that accompanied electrons passing through the collector aperture were returned to the collector circuit by the electric field between the electrodes 10. Unfortunately, our apparatus did not permit the use of potentials large enough to prevent the return of slow negative secondary ions to the target by the action of the magnetic field, or to stop a large group of fast positive ions that reached the collector along with the negative ions. Our values

of the negative ion-ion emission coefficient δ^- are therefore only estimates.

It must be noted that even prolonged thermal conditioning in a high vacuum does not rid the target of nonvolatile impurities. As a second stage of purification preceding all measurements, the working surfaces of targets were bombarded with $\sim 500 \mu\text{a}/\text{cm}^2$ of Ar^+ ions at 30-40 keV. Nonvolatile carbides, silicides, nitrides, and oxides of the different target elements were thus removed from the surface by means of cathode sputtering. The high-temperature targets did not retain deeply penetrating Ar atoms as impurities. (The same

effect is used in separating noble gas isotopes.) The high temperature of the targets also assisted restoration of the regular target-crystal structure after it had been damaged by ion bombardment. Although the ion beam acts catalytically in chemical reactions on a target surface, the targets were not contaminated in our experiments. Early in the 1950's I. M. Samoilov, V. G. Tel'kovskii and the present author showed that the formation rate of impurity film on a molybdenum target is slower than its removal rate for the Ar^+ current density $j > 0.1$ milliamp/cm² with the initial energy $E_0 = 30$ keV and pressure $p < 10^{-6}$ mm Hg.

For the purpose of obtaining reliable reproducible results, Ar^+ bombardment preceded each measurement. This was especially important when measuring the secondary emission coefficient δ^+ for active gas ions (O^+ , N^+ , Cl^+ etc.). When 30-keV Ar^+ were used our purity criterion for the target working surface was the attainment of a minimum value for δ^+ that could be reproduced from run to run and that did not depend on the bombarding-ion current density over a range of two to three orders of magnitude (with $p \leq (2-3) \times 10^{-7}$ mm Hg and $T = 1000^\circ\text{C}$). Further elevation of target temperature would not improve the working surface, since increasing migration rates of impurities from target areas unpurified by the beam and impurity diffusion from the interior would nullify the purifying effect of ion bombardment.

The absolute values of the ion-ion emission coefficient obtained in different runs did not always agree even after careful target preparation. The ionic purification technique enabled us to compare data from different runs. The results for any given series were expressed in relative units with the ion-ion emission coefficient for 30-keV Ar^+ ions taken as unity. Smooth curves then fitted the results of many runs with greatly reduced spread.

The ion-ion emission coefficient of either sign (δ^\pm) will be understood to mean the ratio of the total ion current of the given sign leaving the target during ion bombardment to the current of bombarding ions. Figures 3 to 5 show the coefficients δ^+ as functions of primary ion velocity. Our measured coefficients thus take into account both the current of reflected ions and the current of ionized atoms knocked out of the target surface. Our definition pertains to ion currents rather than to numbers of ions, since it is a very complicated problem to determine the numbers of ions with different masses and overlapping energy spectra and in different stages of ionization. For the same reason the distinguishing of reflected ions from all other secondary ions according to their energies, as in reference 9, for example, does not achieve its purpose in most instances; it does not represent correctly the true ratio between the numbers of secondary ions formed in different ways.

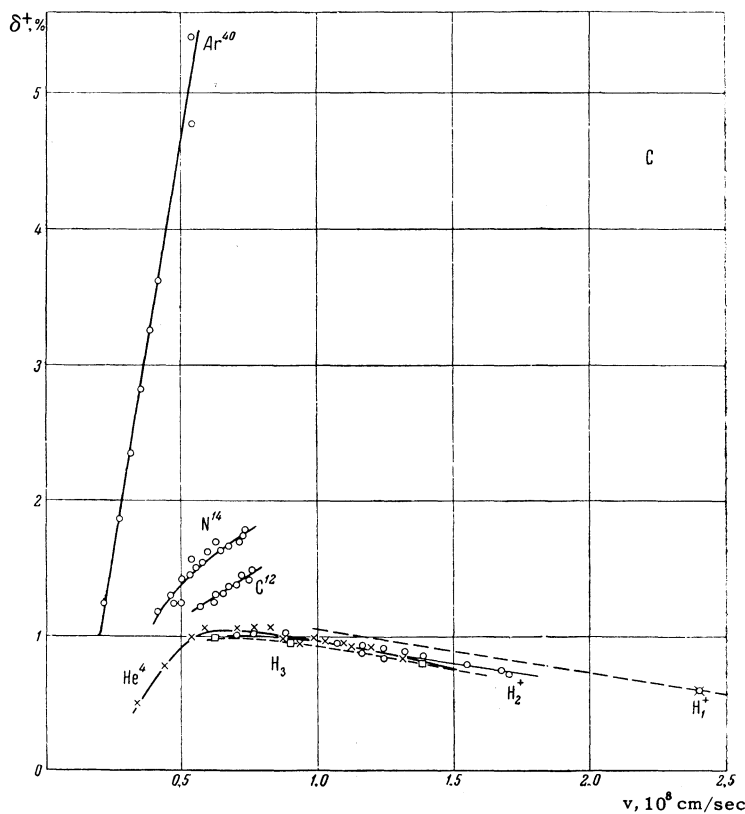


FIG. 5. Ion-ion emission coefficient $\delta^+(v_0)$ for graphite target bombarded with Ar^+ , N^+ , C^+ , H_1^+ , H_2^+ , and H_3^+ ions. For H_3^+ , $\frac{1}{3}\delta$ is given; for H_2^+ , $\frac{1}{2}\delta$ is given.

RESULTS

Before the measurements of δ^+ were begun, a special experimental run investigated the dependence of secondary-ion emission on the gas pressure around the target, on target temperature, and on the primary ion current density. It was found that at pressures below $2-3 \times 10^{-7}$ mm and at 1300°K , δ^+ for pure Mo and Zr targets is independent of the incident ion current density. All curves in Figs. 3–5 were obtained under these conditions.

The most complete studies were carried out for secondary ion emission from Mo (containing 0.008% Fe and 0.007% Al), Zr (obtained by the iodide decomposition process), and graphite (EG-14) bombarded with H_1^+ , H_2^+ , H_3^+ , He^+ , C^+ , N^+ , O^+ , Cl^+ , Ar^+ , and Mo^+ . Even a slightly increased impurity content in the Mo target resulted in an appreciable increase of δ^+ .

In Figs. 3, 4, and 5 the curves of $\delta^+(v_0)$ for all targets are similar. This applies also to copper and molten tin, the data for which are not presented here. It is noteworthy that δ^+ increases proportionately to the velocity of heavy primary ions from 10^7 to 10^8 cm/sec, and that it decreases smoothly at higher velocities of light ions.

Figures 3, 4, and 5 show that with increasing mass of the incident ion secondary-ion emission grows rapidly regardless of whether the bombarding ions are heavier or lighter than the target ions. Secondly, δ^+ also increases with the mass of the target ions. It is found that the secondary-ion currents produced by bombardment with the molecular ions H_2^+ and H_3^+ are almost two and three times greater, respectively, than the secondary-ion current produced by H_1^+ with the same velocity. This agrees well with the hypothesis of many investigators that molecular ions dissociate into their atomic components upon striking a solid surface. In this case the somewhat smaller number of secondary ions produced per atom, compared with the results from bombardment with the corresponding monatomic ions, suggests that a small fraction of molecular ions are reflected without dissociating. This difference could be attributed to a possible difference between the secondary emission coefficients for ions and neutral atoms. However, a special experimental run showed that in our energy range the emission coefficient does not depend on the unneutralized charge of bombarding particles. This effect results from the completely determinate statistically averaged equilibrium charge distribution in a beam of particles with like velocities, traversing even a small number

of atomic layers in a target. Both of our conclusions are in accord with the analogous characteristics of secondary-electron emission under ion bombardment.^[8]

More detailed measurements of $\delta^+(v_0)$ for protons sometimes reveal a fine structure. The smoothness of the $\delta^+(v_0)$ curve for Mo is broken by a sharp decline of ion emission at H_1^+ velocities around 1.4×10^8 , 1.7×10^8 , and 2.8×10^8 cm/sec. In all instances the half-width of the minimum was not greater than 0.5 keV.

The measurements indicated that $\delta^-(v_0)$ varies in the same way as $\delta^+(v_0)$, and that the respective absolute values are of the same order of magnitude. The curves for $\delta^-(v_0)$ are not given here because of their low accuracy. The resemblance between $\delta^-(v_0)$ and $\delta^+(v_0)$ suggests that $\delta^0(v_0)$ will vary in a similar manner. (Some ions can be reflected in the neutralized state.)

We can therefore assume identical mechanisms for secondary-ion emission and cathode sputtering in a high vacuum with bombarding currents that do not greatly elevate the temperature of the entire target. The relative numbers of particles can vary depending on the amount and character of metal surface contamination and the probabilities for the formation and neutralization of all kinds of emitted particles in each energy interval.

It is difficult to compare our present data with the existing theories of cathode sputtering, which do not allow for the possibility that sputtering products will be ionized. Nevertheless, the positions of the peaks on the $\delta^+(v_0)$ curves for H_1^+ bombardment of Mo and Zr can be regarded as confirming Keywell's^[2] hypothesis regarding the interaction of bombarding ions with lattice atoms and conduction electrons in metals.

In conclusion the author wishes to thank L. A. Artsimovich, I. N. Golovin, and G. Ya. Shchepkin for their continued interest and valuable discussions, V. G. Tel'kovskii for several useful comments, and laboratory assistants A. A. Borisov and Yu. E. Pavlov for assistance with the apparatus.

¹ H. Massey and E. Burhop, *Electronic and Ionic Impact Phenomena*, Clarendon Press, Oxford, 1952.

² F. Keywell, *Phys. Rev.* **97**, 1611 (1955).

³ D. E. Harrison, *Phys. Rev.* **102**, 1473 (1956).

⁴ D. T. Goldman and A. Simon, *Phys. Rev.* **111**, 383 (1958).

⁵ O. von Roos, *Z. Physik* **147**, 184 (1957).

⁶ K. Thommen, *Z. Physik* **151**, 144 (1958).

⁷ Craston, Hancox, Robson, Kaufman, Miles, Ware, and Wesson, *Proc. 2nd International Con-*

ference on the Peaceful Uses of Atomic Energy, Geneva, 1958, vol. 32, p. 414.

⁸ V. G. Tel'kovskii, Doklady Akad. Nauk SSSR **108**, 446 (1956), Soviet Phys.-Doklady **1**, 334 (1957).

⁹ Fogel', Slabospitskii, and Rastrepin, J. Tech. Phys. (U.S.S.R.) **30**, 63 (1960), Soviet Phys.-Tech. Phys. **5**, 58 (1960).

¹⁰ F. Seitz and D. Turnbull, editors, Solid State Physics, Academic Press, Inc., New York, 1958.

¹¹ R. L. Hines and R. Arndt, Phys. Rev. **119**, 623 (1960).

Translated by I. Emin

1